FULL PAPER

Dalton
www.rsc.org/dalton

Internal hydrogen bonding and amide co-ordination in zinc(II) complexes of a tripodal N4 ligand: structural, spectroscopic and reactivity studies †

Juan C. Mareque Rivas,* Rafael Torres Martín de Rosales and Simon Parsons
School of Chemistry, The University of Edinburgh, Joseph Black Building, King's Buildings, West Mains Road, Edinburgh, UK EH9 3JJ. E-mail: Juan.mareque@ed.ac.uk

Received 11th February 2003, Accepted 3rd April 2003
First published as an Advance Article on the web 22nd April 2003

The tripodal N4 ligand *N,N*-bis(2-pyridylmethyl)-*N*-(6-pivaloylamido-2-pyridylmethyl)amine (bppapa) presents an N–H group for hydrogen bonding to an adjacent metal-bound ligand, and a carbonyl group for metal co-ordination. These binding features are key in metallopeptidase catalysis, which is an area of considerable current interest. The X-ray crystal structure and ^{1}H NMR studies of bppapa show an intramolecular C–H ··· O=C interaction involving the pivaloylamido unit that determines the orientation of the amide N–H and C=O groups relative to the N4 metal binding site. The reaction of $[Zn(NCCH_3)_4](PF_6)_2$ with bppapa affords $[(bppapa)Zn](PF_6)_2$ **1**. The X-ray crystal structure of **1**·0.5CH_3OH shows a zinc(II) ion in a trigonal-bipyrimidal environment in which the bridgehead nitrogen atom of the ligand and the carbonyl oxygen of the pivaloylamido group co-ordinate axially. ^{1}H and ^{13}C NMR and IR spectra show that this structure is retained in acetonitrile solution. The reaction of $ZnCl_2$ with bppapa in acetonitrile affords the salt [(bppapa)Zn(Cl)](Cl) **2**, which in methanol undergoes anion metathesis with $NaBPh_4$ (1 equiv.) to form [(bppapa)Zn(Cl)](BPh_4) **2′** and NaCl. The X-ray crystal structure of **2′**·CH_3CN shows that the chloride ion occupies one of the axial co-ordination sites of the trigonal-bipyramidal co-ordination geometry of the zinc(II) center. In addition, this structure reveals internal N–H ··· Cl–Zn, C–H ··· Cl–Zn and C–H ··· O=C hydrogen bonding. Remarkably, all these interactions are retained in solution and are clearly reflected in the ^{1}H NMR spectra, which we prove can be used as a powerful diagnostic tool for determining the solution structures of these and related metal complexes. IR spectroscopy was used to determine the strength of the N–H ··· Cl hydrogen bond, which was estimated to be at least 10.3 ± 0.6 kJ mol^{-1} in acetonitrile solution and 14.9 ± 0.6 kJ mol^{-1} in the solid state. The $[(bppapa)Zn(Cl)]^+$ cation is very stable to substitution of the chloride ion by water, which may be an indication of the stabilising effect exerted by internal hydrogen bonding.

Introduction

The involvement of well-positioned YH groups (Y = N, O) of arginine, lysine, histidine, tyrosine and/or serine residues in hydrogen bonding interactions to water and/or substrate groups in zinc peptidases and amidases is common (Scheme 1).[1] Some examples include carboxypeptidase A,[2] aminopeptidase A,[3] the lethal anthrax factor (LF),[4] thermolysin,[5] *Pseudomonas aeruginosa* alkaline protease,[6] and several matrix metalloproteinases.[7] In these enzymes, in addition to the metal(s), commonly zinc(II), the participation of these active-site residues in proton transfer events, peptide (substrate) binding, positioning and activation, activation of water (nucleophile), and transition state stabilisation may be essential. Moreover, the co-operation between metals and non-co-ordinating active-site residues may be necessary for the efficient activation, recognition and/or stabilisation mechanisms displayed by these important enzymes. The relative contribution of metal ions and aforementioned active site residues to the activity of peptidases, however, remains to be elucidated.

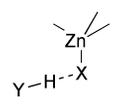

Y = O, N; X = H_2O, OH, peptide

Scheme 1

The identification and implementation of strategies for inducing hydrogen bonding to metal-bound ligands is one of the requirements prior to being able to elucidate the relative contribution of metals and second sphere residues in peptidases using synthetic models. Another important requirement is finding a reliable method to obtain structural information in solution, and so unambiguously establish the formation and strength of the desired second sphere hydrogen bonding interactions. It should then be possible to quantify the relative contribution of the metal and hydrogen bonding by correlating the strength of hydrogen bonding with the rate of hydrolysis.

Here, we demonstrate the validity of positioning amide N–H groups adjacent to a co-ordinating pyridine nitrogen atom as a strategy to achieve hydrogen bonding to another metal-bound ligand, in this case a chloride ion. We provide a simple and reliable method based on NMR and IR studies, which establishes the formation of these hydrogen bonds in solution and determines their strength. Recently, we used related studies to investigate hydrogen bonding in a synthetic model for the K^+-channel.[8]

Hydrogen bonding to metal bound ligands is an area of considerable interest. Research over the past five years has shown that metal-bound chlorides are excellent hydrogen bond acceptors.[9] Metal chlorides are common pro-drugs that are activated by hydrolysis of the metal chloride to a metal water/hydroxide [10] and here we consider the effect that hydrogen bonding has on the stability of the zinc(II)–chloride bond.

Several studies have also demonstrated the importance of hydrogen bonding in the chemistry of other metal co-ordinated anions.[11] In addition, a number of very interesting studies have shown recently the importance of incorporating second sphere residues in synthetic models of other zinc(II) enzymes

† Electronic supplementary information (ESI) available: ORTEP plots of bppapa and **1**·0.5MeOH showing hydrogen bonding; ^{1}H NMR spectra of **1**, **1** with $Me_4NOH·5H_2O$ over time and bppapa with $Me_4NOH·5H_2O$ over time. See http://www.rsc.org/suppdata/dt/b3/b301651j/

DOI: 10.1039/b301651j

including lyases,[12] nucleases,[13] phosphoryl transferases,[14] oxidoreductases.[15]

Another key aspect to consider in synthetic modelling chemistry of metalloenzymes is the fact that although Nature delivers substrates to enzyme active sites with ease and precision this exercise can present a significant challenge to chemists, particularly if labile metals are involved, as is the case in metallopeptidases. Thus, the mechanisms of peptide hydrolysis depend on the way in which amide groups bind at the active site and/or to the metal centre, and their reaction with water/hydroxide species (metal bound or unbound) (Scheme 2).[16] The extent to which we can mimic and/or learn about the mechanisms of hydrolysis in metallopeptidases with synthetic models relies on the ability to mimic and/or induce binding of an amide oxygen to a labile metal centre such as zinc(II).

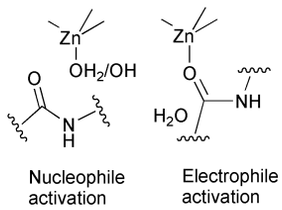

Scheme 2

The covalent attachment of an amide unit adjacent to a ligating atom is a useful strategy to induce co-ordination of its carbonyl group to a labile metal.

Results and discussion

Design and synthesis

The tripodal N4 ligand *N,N*-bis(2-pyridylmethyl)-*N*-(6-pivaloylamido-2-pyridylmethyl)amine (bppapa) (Scheme 3) provides a good ligand platform for mimicking several key active site features of peptidases and amidases including co-ordination of the amide carbonyl group, a peptide (amide) bond and a metal-bound water/hydroxide molecule brought into close proximity of one another, and hydrogen bonding to zinc-bound water/hydroxide.

From a co-ordination chemistry point of view, the N4 binding site provided by bppapa can be used as a source of stability for the resulting zinc(II) complexes, while it leaves available co-ordination sites to exogenous ligands *e.g.* water molecules and hydroxide ions. In addition, because bppapa positions an amide N–H group in close proximity to adjacent metal

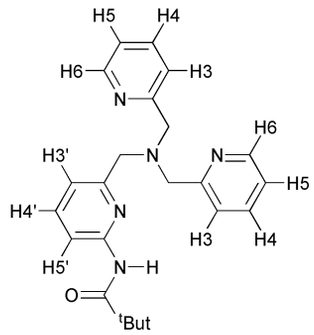

bppapa

Scheme 3

binding sites, metal complexes of bppapa could be relevant to assessing the contribution of hydrogen bonding to the hydroxide mechanism of peptidases. Since bppapa also positions a carbonyl group in close proximity to the metal binding site, metal complexes of bppapa and related ligands could be used as models for assessing the effectiveness of the carbonyl mechanism proposed for peptidases.[16]

The synthesis of the zinc(II) complexes $[(bppapa)Zn](PF_6)_2$ **1** and [(bppapa)Zn(Cl)](X) (**2**, X = Cl; **2′**, X = BPh_4) was accomplished using $ZnCl_2$ as common precursor. Thus, the reaction of $ZnCl_2$ with two equivalents of $AgPF_6$ in dry acetonitrile affords the $[Zn(NCCH_3)_4](PF_6)_2$, which after removal of the AgCl by filtration and addition of one equivalent of bppapa affords **1**. The $[(bppapa)Zn]^{2+}$ cation can be quantitatively converted to the $[(bppapa)Zn(Cl)]^+$ cation in the presence of Cl^- ions. Alternatively, the $[(bppapa)Zn(Cl)]^+$ cation can be prepared from the reaction of equimolar amounts of bppapa and $ZnCl_2$ in acetonitrile (Scheme 4).

X-Ray crystallography

Crystal data for bppapa, **1**·0.5CH_3OH and **2′**·CH_3CN are listed in Table 1.

Structure of bppapa. An ORTEP plot[17] of the X-ray crystal structure of bppapa is shown in Fig. 1. In this structure the three pyridine nitrogens (N(2), N(12) and N(22)) are located on the same side of the molecule, and opposed to the bridgehead amine nitrogen (N(1)) of the tripodal ligand (Fig. 1). Presumably this arrangement allows a weak interaction between the H-atoms in the 3-position of each pyridine ring and the lone pair of the bridgehead nitrogen. It allows also the amide N–H

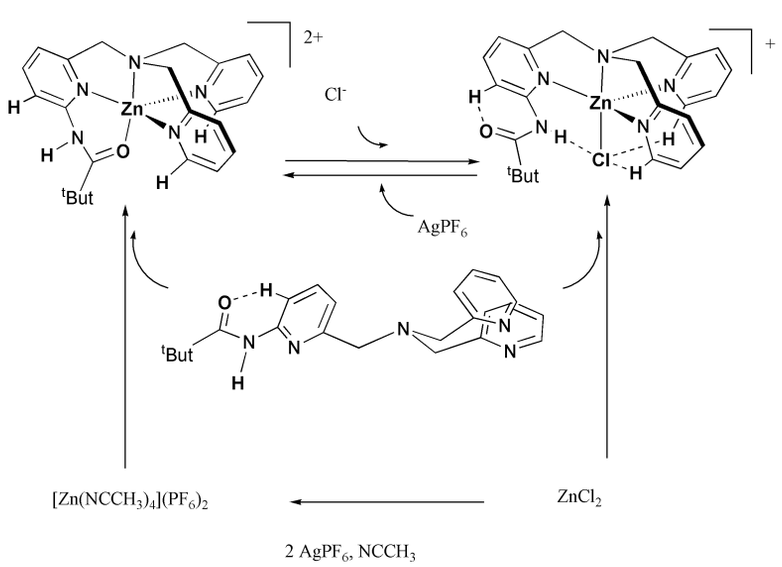

Scheme 4

Table 1 Crystallographic data and structure refinement details for bppapa and complexes **1**·0.5CH_3OH and **2′**·CH_3CN

	bppapa	**1**·0.5CH_3OH	**2′**·CH_3CN
Empirical formula	$C_{23}H_{27}N_5O$	$C_{23.50}H_{29}F_{12}N_5O_{1.50}P_2Zn$	$C_{49}H_{50}BClN_6OZn$
M	389.50	760.83	850.58
T/K	150	150	150
Crystal system	Monoclinic	Monoclinic	Triclinic
Space group	$P2_1/c$	$P2_1/c$	$P\bar{1}$
Crystal size/mm	0.63 × 0.34 × 0.27	0.5 × 0.29 × 0.12	0.86 × 0.42 × 0.26
a/Å	10.9702(9)	14.424(2)	10.295(3)
b/Å	9.7048(8)	11.3946(19)	14.243(4)
c/Å	19.1103(15)	19.420(2)	15.328(4)
α/°	90.00	90.00	73.973(5)
β/°	90.555(2)	106.072(11)	86.034(5)
γ/°	90.00	90.00	84.577(5)
V/Å^3	2034.5(3)	3067.0(8)	2148.4(11)
Z	4	4	2
D_{calc}/g cm^{-3}	1.272	1.648	1.315
μ/mm^{-1}	0.081	3.062	0.679
Reflections measured, unique	12533, 4928	7387, 5451	19695, 10161
R_{int}	0.0259	0.0256	0.0247
$R_1(F)$ [a]	0.0566	0.0419	0.0502
$wR_2(F^2)$ [a] (all data)	0.1221	0.0770	0.0983
$S(F^2)$ [a] (all data)	1.018	1.028	0.953
Largest difference peak, hole/e Å^3	0.365, −0.228	0.423, −0.327	0.544, −0.304

[a] $R_1(F) = \Sigma(||F_o| - |F_c||)/\Sigma(|F_o|)$; $wR_2(F^2) = [\Sigma w(F_o^2 - F_c^2)^2/\Sigma wF_o^4]^{1/2}$; $S(F^2) = [\Sigma w(F_o^2 - F_c^2)^2/(n-p)]^{1/2}$.

Table 2 Geometric features of the main hydrogen bonding interactions in bppapa, **1**·0.5CH_3OH and **2′**·CH_3CN [a]

Interaction	D–H/Å	D ··· A/Å	H ··· A/Å	D–H ··· A/°
bppapa				
N(7)–H(7N) ··· N(12)[c]	1.01[a]	3.2720(15)	2.33	154.4
1·0.5CH_3OH				
N(7)–H(7N) ··· F(13)	1.01[a]	3.472(3)	2.56	149.7
N(7)–H(7N) ··· F(16)	1.01[a]	3.310(2)	2.46	141.7
C(5)–H(5) ··· F(13)	0.95[a]	3.391(3)	2.59	142.2
C(5)–H(5) ··· F(15)	0.95[a]	3.257(3)	2.34	161.0
C(5)–H(5) ··· F(16)	0.95[a]	3.433(3)	2.65	140.1
2′·CH_3CN				
N(7)–H(7N) ··· Cl	1.01[b]	3.2127(19)	2.22	167.7
C(16)–H(16A) ··· Cl	0.95[a]	3.348(2)	2.77	119.8
C(26)–H(26A) ··· Cl	0.95[a]	3.566(3)	2.98	120.9
C(10C)–H(10H) ··· Cl	0.95[a]	3.716(2)	2.80	156.0

[a] Fixed distance and calculated position. [b] Extended distance. [c] Generated applying the symmetry operation $-x, 0.5 + y, 0.5 - z$.

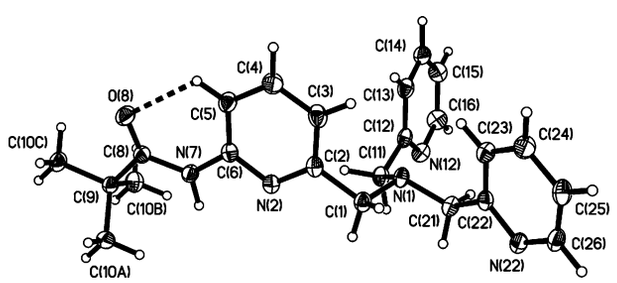

Fig. 1 An ORTEP plot drawn with 50% probability thermal ellipsoids of ligand bppapa.

to be engaged in hydrogen bonding with a pyridine nitrogen of a symmetry related molecule in the crystal structure (Table 2, Fig. S1 (see ESI †)). In this arrangement, however, a substantial re-organisation needs to take place to allow metal co-ordination to the three pyridine (N_{py}) and one amine (N_{amine}) nitrogen atoms.

The amide plane of the pivaloylamido unit in bppapa is oriented in such a way as to optimise the interaction of its oxygen with the hydrogen atom in the adjacent position of the same pyridine ring, namely H5 (C(5) ··· O(8) 2.8174(16) Å, H(5A) ··· O(8) 2.22 Å, C(5)–H(5A) ··· O(8) 120° with C(5)–H(5A) fixed to 0.95 Å). In agreement with this suggestion is the small angle between the pyridine (N(2)C(2)C(3)C(4)C(5)C(6)) and amide (N(7)C(8)O(8)) planes, 11.4°. In this arrangement, the amide N–H is optimally pre-organised for the interaction with molecules '*cis*' to the pyridine N-atom once bound to a metal (*vide infra*).

Structure of [(bppapa)Zn](PF$_6$)$_2$ 1·0.5CH$_3$OH. Single crystals suitable for X-ray diffraction were grown by slow evaporation of a solution of [(bppapa)Zn](PF$_6$)$_2$ **1** in methanol/chloroform (1 : 1). The structure of the cation is shown in Fig. 2 and selected distances and angles are given in Table 3. The zinc(II) center is in a trigonal bipyramidal N4O environment with the three pyridine nitrogen atoms occupying the equatorial positions and the bridgehead nitrogen and amide oxygen in the axial positions. A related structure with the zinc(II) center in a N2S2O co-ordination environment was reported recently.[18] In **1**, the zinc(II) ion sits slightly above the trigonal 'plane' resulting in acute N_{axial}–Zn–$N_{equatorial}$ angles of 80.12(7)°, 81.09(7)° and 80.01(7)°. The Zn–N_{py} distances are 2.060(2) Å, 2.023(2) Å and 2.027(2) Å, the longest corresponding to the substituted pyridine, presumably due to the electron-withdrawing effect of the pivaloylamido

Table 3 Selected bond lengths (Å) and angles (°) for zinc(II) complexes **1**·0.5CH_3OH and **2′**·CH_3CN

	1·0.5CH_3OH	**2′**·CH_3CN
Zn–N(2)	2.0590(18)	2.1351(15)
Zn–N(12)	2.0227(19)	2.0885(16)
Zn–N(22)	2.0272(19)	2.0651(17)
Zn–N(1)	2.1750(18)	2.1990(15)
Zn–O(8)	2.0005(16)	N/A
Zn–Cl	N/A	2.2812(7)
N(2)–Zn–N(12)	118.08(8)	121.11(6)
N(2)–Zn–N(22)	123.53(7)	109.84(6)
N(12)–Zn–N(22)	110.12(8)	115.84(6)
N(1)–Zn–N(2)	80.12(7)	78.02(5)
N(1)–Zn–N(12)	81.09(7)	77.51(6)
N(1)–Zn–N(22)	80.01(7)	77.75(6)
N(1)–Zn–O(8)	167.75(6)	N/A
N(1)–Zn–Cl	N/A	174.09(4)
O(8)–Zn–N(2)	88.59(7)	N/A
O(8)–Zn–N(12)	108.69(7)	N/A
O(8)–Zn–N(22)	102.67(7)	N/A
Cl–Zn–N(2)	N/A	106.20(4)
Cl–Zn–N(12)	N/A	96.66(5)
Cl–Zn–N(22)	N/A	104.24(5)

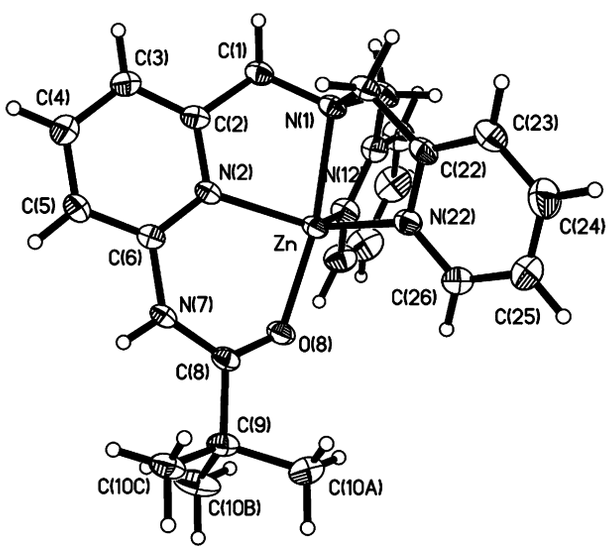

Fig. 2 An ORTEP plot drawn with 50% probability thermal ellipsoids of the molecular structure of the $[(bppapa)Zn)]^{2+}$ cation of **1**·0.5CH_3OH.

unit. The Zn–N_{amine} distance of 2.175(2) Å is significantly longer than the Zn–N_{py} distances. The angle between the atoms located at the axial positions, N(1)–Zn–O(8) is 167.75(6)° and bent towards the substituted pyridine. This deviation from linearity and orientation presumably optimises co-ordination of the carbonyl group. The amide NH and the adjacent aromatic CH hydrogen bond to one of the PF_6^- molecules in a polyfurcated mode (Table 2, Fig. S2 (see ESI †)).

Structure of [(bppapa)Zn(Cl)](BPh$_4$) 2′·CH$_3$CN. Single crystals suitable for X-ray diffraction were grown by slow evaporation of a solution of **2′** in CH_3CN/H_2O (1 : 1). The structure of the $[(bppapa)Zn(Cl)]^+$ cation is shown in Fig. 3; selected distances and angles are given in Table 3. As in **1**, the zinc(II) centre is in a trigonal bipyramidal environment ligated to the three pyridine nitrogen atoms in the trigonal plane, and to the bridgehead nitrogen of the tripodal ligand and a chloride ion in the axial positions. Co-ordination of the chloride dictates the positioning of the pivaloylamido group, which seeks to optimise N–H ··· Cl hydrogen bonding (N(7) ··· Cl 3.2127(19) Å; H(7N) ··· Cl 2.22 Å; N(7)–H(7N) ··· Cl 168° for a N(7)–H(7N) bond extended to 1.01 Å).[19] As a result of this, the angle between the pyridine plane (N(2)C(2)C(3)C(4)C(5)C(6)) and

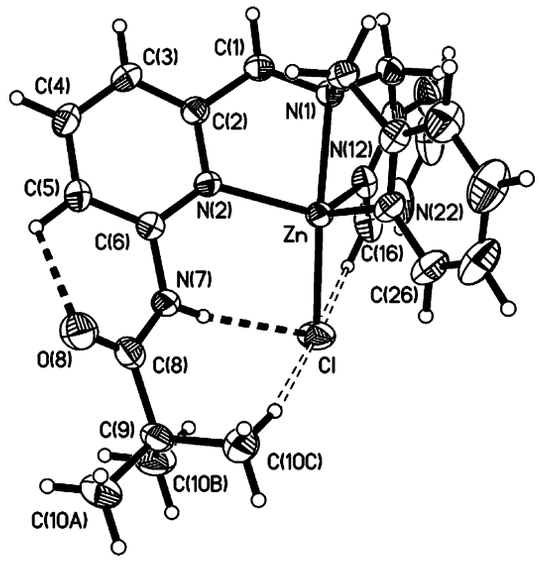

Fig. 3 An ORTEP plot drawn with 50% probability ellipsoids of the molecular structure of the $[(bppapa)Zn(Cl)]^+$ cation of **2′**·CH_3CN.

the plane containing the amide group (N(7)C(8)O(8)) is 31.5°. This arrangement of the amide group, however, still allows some interaction between the carbonyl O-atom and H5, (C(5) ··· O(8) 2.83(3) Å, H(5A) ··· O(8) 2.34 Å, C(5)–H(5A) ··· O8 112° with C(5)–H(5A) fixed to 0.95 Å) although this is slightly weaker than in 'free' bppapa. As in **1**, the longest Zn–$N_{equatorial}$ bond is made to the substituted pyridine. All Zn–N distances are longer than the corresponding ones in **1** and are in accordance with other $[(L)Zn(Cl)]^+$ cations,[20] which may reflect a combination of electronic and steric effects associated with co-ordinating the chloride ion at the axial position and the different arrangement of the pivaloylamido group. Thus, the zinc(II) center in **2′**, which is part of a 1+ cation, should be more electron rich than in **1**, in which it is part of a 2+ cation. Also, the fact that all N_{axial}–Zn–$N_{equatorial}$ angles, 78.02(5)°, 77.51(6)° and 77.75(6)°, are smaller than in **1** may be an indication of a more sterically demanding arrangement of the pivaloylamido group.

Another interesting feature of the X-ray crystal structure of **2′** is intramolecular C–H ··· Cl hydrogen bonding. The zinc-bound chloride interacts weakly with hydrogen atoms of the *tert*-butyl group and the *ortho* position (6-position) of the one of the pyridines (Table 2, Fig. 3). Interaction with the pyridine hydrogen atoms may be facilitated by the N_{amine}–Zn–Cl angle of 174.09(4)°, which is significantly more linear than the N_{amine}–Zn–O angle in $[(bppapa)Zn]^{2+}$ (167.75(6)°), bringing the co-ordinated chloride closer to the *ortho* (6-position) pyridine hydrogen atoms.

Thus, in **2′** N–H ··· Cl, C–H ··· Cl and C–H ··· O hydrogen bonding seem to be in balance and in which N–H ··· Cl hydrogen bonding is the strongest. The subtle balance or competition of intermolecular interactions determines their relative strength.[21]

NMR and IR studies

^{1}H NMR studies of bppapa in acetonitrile reveal a downfield shift of the H5′ resonance relative to H3′, which is consistent with the retention of the C–H ··· O interaction in solution. In **1** all the ^{1}H NMR resonances undergo a downfield shift relative to bppapa, consistent with metal binding. A notable exception is the shift by 0.55 ppm upfield of H5′ (Fig. 4, Table 4). This upfield proton chemical shift is consistent with breaking the C–H5′ ··· O=C interaction. In **2′** most aromatic resonances are shifted upfield by 0.1–0.3 ppm compared to those in **1**, a feature consistent with a more electron rich zinc(II) centre in **2′**. The notable exceptions, however, are H6, H5′ and the N–H,

Table 4 Summary of ^{1}H NMR (360 MHz, CD_3CN, 293 K) chemical shift data for bppapa, **1** and **2′** [a]

	bppapa	**1**	**2′**
^{t}Bu			
H10	1.26	1.54 (+0.28)	1.37 (−0.17)
NH			
H7	8.16	9.48 (+1.32)	10.67 (+1.19)
$PyCH_2N$			
$H1'_{A,B}$	3.71	4.28 (+0.57)	4.03 (−0.25)
$H1_{A,B}$	3.79	4.32 (+0.53)	4.10 (−0.22)
py (aromatic)			
H3′	7.32	7.38 (+0.06)	7.12 (−0.26)
H4′	7.67	8.10 (+0.43)	7.92 (−0.18)
H5′	7.98	7.43 (−0.55)	8.32 (+0.89)
H3	7.60	7.61 (+0.01)	7.50 (−0.11)
H4	7.70	8.12 (+0.42)	8.05 (−0.07)
H5	7.18	7.67 (+0.49)	7.62 (−0.05)
H6	8.47	8.57 (+0.10)	9.03 (+0.46)

[a] Chemical shifts are in ppm relative to CH_3CN at 1.94 ppm. Values in parentheses denote chemical shifts downfield (positive) or upfield (negative) *versus* values in previous column. The symbol ′ refers to the 2-pyridylmethyl with the 6-pivaloylamido group.

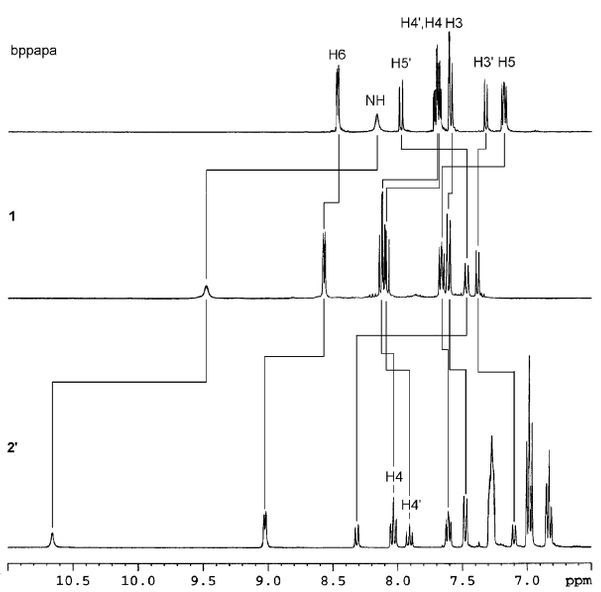

Fig. 4 Aromatic and NH region of the ^{1}H NMR spectrum (360.1 MHz, CD_3CN, 293 K) of bppapa (top), **1** (middle) and **2′** (bottom). See Table 3 for chemical shift values and Scheme 3 for labelling scheme explanation.

which undergo large downfield shifts of *ca.* 0.4–1.2 ppm (Fig. 4, Table 4). These downfield shifts can be rationalised in terms of the N–H7 ··· Cl–Zn, C–H6 ··· Cl–Zn and C–H5′ ··· O=C hydrogen bonding interactions found in the X-ray crystal structure of **2′** being retained in solution. It is particularly remarkable that the C–H ··· Cl hydrogen bonding interactions are retained in solution as to our knowledge these interactions have only been previously claimed in the solid state. It is also interesting that, despite being considered very weak, C–H ··· Cl–Zn interactions seem to be responsible for quite large downfield shifts of the proton resonances, *ca.* 0.46 ppm. The C–H ··· Cl–Zn hydrogen bonding in **2′** seems to be strong enough to be retained even at high temperatures as suggested by variable temperature (20–50 °C) ^{1}H NMR studies.[22] In addition, the ^{13}C NMR spectra of **1** and **2′** show carbonyl resonances at 185.7 and 178.9 ppm, respectively, which is indicative of the carbonyl group being co-ordinated to the zinc(II) centre in **1** but not in **2′**.

Table 5 Selected infrared vibrational data of **1** and **2′**

	ν_{N-H} [a]/cm^{-1}	$\nu_{C=O}$ [a]/cm^{-1}
[(bppapa)Zn]$(PF_6)_2$ **1** (CH_3CN solution)	3328	1625
[(bppapa)Zn(Cl)](BPh_4) **2′** (CH_3CN solution)	3263	1700
(**2′** − **1**)	(−65)	(75)
[(bppapa)Zn]$(PF_6)_2$ **1** (solid state)	3390	1624
[(bppapa)Zn(Cl)](BPh_4) **2′** (solid state)	3255	1700
(**2′** − **1**)	(−135)	(76)

[a] ± 4 cm^{-1}.

IR studies are in total agreement with all the conclusions derived from NMR and X-ray studies. Thus, the IR spectra of **1** and **2′** show $\nu_{C=O}$ bands shifted to higher wavenumbers by 75 ± 4 cm^{-1} in acetonitrile solutions and by 76 ± 4 cm^{-1} in the solid state on going from chloride co-ordination in **2′** to amide co-ordination in **1** (Table 5). The N–H ··· Cl–Zn hydrogen bonding is reflected in the ν_{N-H} bands being shifted by 65 ± 4 cm^{-1} in acetonitrile solutions and by 135 ± 4 cm^{-1} in the solid state to lower wavenumbers. These shifts correspond to hydrogen bond energies of at least 10.3 ± 0.6 and 14.9 ± 0.6 kJ mol^{-1}, respectively.[23] The difference between the strength of N–H ··· Cl–Zn hydrogen bonding in solution and the solid state may be due to the balancing with C–H ··· O=C and C–H ··· Cl–Zn interactions, which would result from slight rotation of the amide group and adjustments in the position of the pyridine rings.

Reactivity studies

One of the possible effects of hydrogen bonding to metal bound ligands is to affect their relative stability and reactivity. The [(bppapa)Zn(Cl)]$^+$ cation is formed when equimolar amounts of $ZnCl_2$ and bppapa are mixed in acetonitrile. Addition of a mixture of Cl^- (1 equiv.) in the presence of excess H_2O (60 equiv.) to an acetonitrile solution of [(bppapa)Zn]$^{2+}$ (1 equiv.) affords [(bppapa)Zn(Cl)]$^+$ quantitatively. These reactivity features indicate that chloride- but not water-co-ordination is favoured over the chelate effect associated with amide oxygen co-ordination. Moreover, the [(bppapa)Zn(Cl)]$^+$ is stable to hydrolysis leading to a zinc(II) water/hydroxide. The addition of excess $AgPF_6$ to [(bppapa)Zn(Cl)]$^+$ does, however, result in the formation of AgCl and [(bppapa)Zn]$^{2+}$.[24] These experiments suggest that chloride binding to zinc(II) is favoured over water binding. In principle, internal H-bonding interactions could contribute to the stabilisation of the zinc(II) chloride complex. Thus, it has been shown that metal-bound chlorides are excellent hydrogen bond acceptors.[9] Hydrolysis of metal chlorides is relevant to metallodrug research in that metal chlorides are often used as pro-drugs, which are activated upon hydrolysis of the metal chloride to a metal water/hydroxide. One metallodrug that follows this activation mechanism is cisplatin.[10]

Addition of $Me_4NOH{\cdot}5H_2O$ (1 equiv.) to [(bppapa)Zn]-$(PF_6)_2$ affords [(bppapa^{1-})Zn](PF_6), Me_4NPF_6 and H_2O (6 equiv.), suggesting that co-ordination of the carbonyl group facilitates N–H deprotonation, an event that potentially results in even stronger binding of the amide oxygen. This aspect may be important in determining the rate and mechanism of hydrolysis of peptides, particularly whenever co-ordination of the amide carbonyl group of the scissile bond is involved.[25,26]

Conclusion

This study has explored the validity of the covalent attachment of a pivaloylamido group adjacent to a metal ligating pyridine nitrogen as useful strategy to induce hydrogen bonding to another metal-bound ligand, and to achieve co-ordination of the carbonyl amido group. The study involved a labile metal

center such as zinc(II), which is the most commonly used metal in biological hydrolases. The X-ray crystal structures of the tripodal ligand *N*,*N*-bis(2-pyridylmethyl)-*N*-(6-pivaloylamido-2-pyridylmethyl)amine (bppapa) and two of its zinc(II) complexes, $[(bppapa)Zn](PF_6)_2$ **1** and $[(bppapa)Zn(Cl)](BPh_4)$ **2′** were reported. Carbonyl amide co-ordination and intramolecular N–H ··· Cl–Zn are found in the solid state structures of **1** and **2′**, respectively. After analysing the solid state structures we conclude that a variety of H-bonding interactions are important in defining the molecular structure. This includes intramolecular C–H ··· O=C and C–H ··· Cl–Zn hydrogen bonding interactions.

The emphasis of this study, however, was on correlating solid state and solution structures. The studies reported herein provide good evidence that all structural features found in the solid state structures are retained in solution and are clearly expressed in the ^{1}H, ^{13}C NMR and IR spectra of these compounds. Moreover, this work reveals the characteristic ^{1}H NMR signatures of each of these two possible arrangements of the pivaloylamido unit, namely internal and external N–H, which can be used as a diagnostic tool for postulating the structures of ligands with a 6-amidopydinemethylamine unit. We also report that C–H ··· Cl–Zn hydrogen bonding in **2′** results in large proton chemical shift changes. C–H ··· Cl–M (M = transition metal) hydrogen bonding has received considerable attention,[9] however, this work provides what is to our knowledge the first experimental evidence that these interactions can be retained in solution. In an initial attempt to correlate the aforementioned structural features with reactivity we propose that the ability of metal chlorides to act as strong hydrogen bond acceptors may affect the stability of the metal–chloride bond and make it more resistant to hydrolysis. This initial work suggests also that co-ordination of the carbonyl group facilitates deprotonation of the amide N–H group, which is relevant to hydrolysis of peptide bonds if metal co-ordination is involved.

Experimental

General

Reagents were obtained from commercial sources and used as received unless otherwise noted. Solvents were dried and purified under N_2 by using standard methods[27] and were distilled immediately before use. All compounds were prepared under N_2 unless otherwise mentioned. The tripodal ligand bppapa was prepared adapting a literature procedure used for the synthesis of tris[(6-pivaloylamido)-2-pyridyl)methyl]amine (tppa).[28] The NMR spectra were obtained using Bruker ARX 250 or Bruker ARX 360 spectrometers at 20 °C in CD_3CN unless otherwise noted. ^{13}C and ^{1}H chemical shifts are referenced with respect to the carbon (δ_C 1.32 and 118.26 ppm) and residual proton (δ_H 1.94 ppm) solvent peaks. Peak assignments are done with the aid of 2-D NMR spectroscopy. Sample concentrations for the NMR studies were 0.02–0.04 M. Mass spectra were performed on a micromass Platform II system operating in flow injection analysis mode with the electrospray method. Elemental analyses were carried out by the microanalyses service provided by the School of Chemistry at the University of Edinburgh. Infrared spectra were recorded with a JASCO FTIR-410 spectrometer between 4000 and 250 cm^{-1} as KBr pellets (solid state) or as acetonitrile solutions in KBr cells. Solid state and solution FTIR studies were used to estimate the strength of N–H ··· Cl–Zn H-bonding applying Iogansen's equation.[23]

Synthesis

***N,N*-Bis(2-pyridylmethyl)-*N*-(6-pivaloylamido-2-pyridylmethyl)amine (bppapa).** 2-(Pivaloylamido)-6-(aminomethyl)-pyridine[28] (7 g, 34 mmol) and 2-picolyl chloride (11 g, 68 mmol) were dissolved in acetonitrile (100 cm^3) and stirred at room temperature for 5 minutes. Then, sodium carbonate (36.4 g, 0.34 mol) was added and the temperature was raised to 44 °C. After 48 h the solution was cooled to room temperature and poured into 200 cm^3 of 1 M $NaOH_{(aq)}$. The crude product was then extracted with dichloromethane (3 × 80 cm^3) and the organic fractions were dried over Na_2SO_4. The solvent was evaporated under vacuum to yield the crude product as a brown oil. The crude material was recrystallised from diethyl ether (100 cm^3) to yield the pure product as a dark red solid (7.6 g, 59%) (Found: C, 70.89; H, 6.95; N, 17.86. Calc. for $C_{23}H_{27}N_5O$: C, 70.92; H, 6.99; N, 17.89%). ^{1}H NMR (CD_3CN, 360.1 MHz) δ_H (ppm) 8.47 (dd, *J* = 4.9, 1.9 Hz, 2H, py-*H*6), 8.16 (s, 1H, N*H*), 7.98 (t, *J* = 8.2 Hz, 1H, py′-*H*5), 7.70 (td, *J* = 7.7 and 1.8 Hz, 2H, py-*H*5), 7.69 (t, *J* = 7.8 Hz, 1H, py′-*H*4), 7.60 (d, *J* = 7.7 Hz, 2H, py-*H*3), 7.32 (d, *J* = 7.3 Hz, 1H, py′-*H*3), 7.18 (ddd, *J* = 7.5, 4.9, 1.1 Hz, 2H, py-*H*5), 3.79 (s, 4H, NCH_2-py), 3.71 (s, 2H, NCH_2-py′), 1.26 (s, 9H, C–(CH_3)$_3$). ^{13}C NMR (CD_3CN, 90.5 MHz) δ_C (ppm) 176.4 (*C*=O), 159.0 (py-*C*2), 157.7 and 150.6 (py′-*C*2 and py′-*C*6), 148.3 (py-*C*6), 138.0 (py′-*C*3), 135.8 (py-*C*3), 122.2 and 121.5 (py-*C*4 and py-*C*5), 117.8 and 111.0 (py′-*C*4 and py′-*C*5), 59.3 (N*C*H_2-py), 59.0 (N*C*H_2-py′), 38.8 (*C*–(CH$_3$)$_3$), 25.9 (C–(*C*H$_3$)$_3$). ESI-MS (+ion) Found 390.3 (100%), Calcd. 390.23 (100%) for $[(bppapa)H]^+$, and matches theoretical isotope distribution.

$[(bppapa)Zn](PF_6)_2$ 1. $ZnCl_2$(170 mg, 1.290 mmol) and $AgPF_6$ (650 mg, 2.580 mmol) were dissolved in acetronitrile (60 cm^3) and the solution was stirred for 1 h resulting in the appearance of a white precipitate, AgCl, which was removed by filtration. bppapa (500 mg, 1.290 mmol) was then added and the mixture was allowed to react for 12 h at room temperature. The solution was centrifuged and the solvent evaporated under vacuum to yield the product as a yellow solid (770 mg, 80%) (Found: C, 36.83; H, 3.54; N, 9.21. Calc. for $C_{23}H_{27}N_5OZnP_2F_{12}$: C, 37.09; H, 3.65; N, 9.40%). ^{1}H NMR (CD_3CN, 360.1 MHz) δ_H (ppm) 9.48 (br s, 1H, N*H*), 8.57 (dd, J = 5.4, 1.7 Hz, 2H, py-*H*6), 8.12 (td, *J* = 7.7, 1.7 Hz, 2H, py-*H*4), 8.10 (dd, *J* = 8.0, 7.7 Hz, 1H, py′-*H*4), 7.67 (dd, *J* = 8.0, 5.4 Hz, 2H, py-*H*5), 7.61 (d, *J* = 7.8 Hz, 2H, py-*H*3), 7.43 (d, *J* = 8.0 Hz, 1H, py′-*H*5), 7.38 (d, *J* = 7.7 Hz, 1H, py′-*H*3), 4.32 (s, 4H, NCH_2-py), 4.21 (s, 2H, NCH_2-py′), 1.54 (s, 9H, C–(CH_3)$_3$). ^{13}C NMR (CD_3CN, 90.5 MHz, 298 K) δ_C (ppm) 185.7 (*C*=O) 159.4 (py-*C*2) 158.5 and 157.5 (py′-*C*2 and py′-*C*6), 147.9 (py-*C*6), 143.1 (py′-*C*3), 141.5 (py-*C*3), 125.0 and 124.4 (py-*C*4 and py-*C*5), 120.8 and 115.7 (py′-*C*4 and py′-*C*5), 56.8 (N*C*H_2-py), 56.5 (N*C*H_2-py′), 41.2 (*C*–(CH$_3$)$_3$), 25.7 (C-(*C*H$_3$)$_3$). ESI-MS (+ ion) Found 226.6 (100%), Calcd. 226.57 for $[(bppapa)Zn]^{2+}$, and matches theoretical isotope distribution.

$[(bppapa)Zn(Cl)](Cl)$ 2. bppapa (0.25g, 0.6 mmol) and $ZnCl_2$ (0.08g, 0.6 mmol) were dissolved in dry acetonitrile (15 cm^3). The solution was stirred for 20 h at room temperature. The solvent was then evaporated under vacuum to yield a grey solid (0.27 g, 87%) (Found: C, 52.00; H, 5.11; N, 13.20. Calc. for $C_{23}H_{27}N_5OZnCl_2$: C, 52.54; H, 5.18; N, 13.32%). ^{1}H NMR (CD_3CN, 360.1 MHz) δ_H (ppm) 9.77 (s, 1H, N*H*), 8.93 (d, *J* = 5.4 Hz, 2H, py-*H*6), 7.85 (td, *J* = 7.6, 1.7 Hz, 1H, py-*H*4), 7.83 (d, *J* = 8.4 Hz, 2H, py′-*H*5), 7.44 (t, *J* = 7.7 Hz, 1H, py′-*H*4), 7.41 (dd, *J* = 7.1, 5 Hz, 2H, py-*H*5), 7.35 (d, *J* = 7.9 Hz, 2H, py-*H*3), 6.85 (d, 7.4 Hz, 1H, py′-*H*3), 4.5–4.2 (br, 4H, NCH_2-py), 3.8 (s, 2H, NCH_2-py′), 1.39 (s, 9H, C–(CH_3)$_3$); ^{13}C NMR (CD_3CN, 90.5 MHz, 298 K) δ_C (ppm) 178.1 (*C*=O), 154.7 (py-*C*2) 153.0 and 152.9 (py′-*C*2 and py′-*C*6), 147.7 (py-*C*6), 139.7 (py′-*C*3), 140.2 (py-*C*3), 124.5 and 124.4 (py-*C*4 and py-*C*5), 120.0 and 114.7 (py′-*C*4 and py′-*C*5), 59.3 (N*C*H_2-py), 59.3 (N*C*H_2-py′), 40.2 (*C*–(CH$_3$)$_3$), 27.0 (C–(*C*H$_3$)$_3$). ESI-MS (+ ion) Found 488.2 (100%), Calcd. 488.12 (100%) for $[(bppapa)Zn(Cl)]^+$, and matches theoretical isotope distribution.

[(bppapa)Zn(Cl)](BPh$_4$) 2′. 2 (0.10 g, 0.2 mmol) was dissolved in methanol (5 cm^3). NaBPh$_4$ (0.07 g, 0.2 mmol) was then added and the solution was stirred for 2 h. The white precipitate thus formed was collected by filtration, washed with diethyl ether (2 cm^3), and dried under vacuum (0.11 g, 69%) (Found: C, 68.90; H, 5.80; N, 9.65. Calc. for $C_{48}H_{80}BClN_6OZnCl$, **2′**·CH_3CN: C, 69.19; H, 5.92; N, 9.88%). ^{1}H NMR (CD_3CN, 360.1 MHz) δ_H (ppm) [(bppapa)Zn(Cl)]$^+$ 10.67 (s, 1H, N*H*), 9.03 (d, *J* = 4.9 Hz, 2H, py-*H*6), 8.32 (d, *J* = 8.5 Hz, 1H, py′-*H*5), 8.05 (td, *J* = 7.7 and 1.6 Hz, 2H, py-*H*4), 7.92 (t, *J* = 7.9 Hz, 1H, py′-*H*4), 7.62 (t, *J* = 6.3 Hz, 2H, py-*H*5), 7.50 (d, *J* = 7.8 Hz, 2H, py-*H*3), 7.12 (d, 7.5 Hz, 1H, py′-*H*3), 4.10 (s, 4H, NCH_2-py), 4.03 (s, 2H, NCH_2-py′), 1.37 (s, 9H, C–(CH_3)$_3$); BPh$_4^-$ 7.28 (m, 8H, Ar-*H*2), 6.98 (t, *J* = 7.5 Hz, 8H, Ar-*H*3) and 6.83 (t, *J* = 7.2 Hz, Ar-*H*4). ^{13}C NMR (CD_3CN, 62.9 MHz, 298 K) δ_C (ppm); [(bppapa)Zn(Cl)]$^+$ 178.9 (*C*=O), 155.6 (py-*C*2), 154.9 (py′-*C*2), 154.2 (py′-*C*6), 149.5 (py-*C*6), 143.0 (py′-*C*3), 142.4 (py-*C*3), 126.1 (py-*C*4), 125.6 (py-*C*5), 120.3 (py′-*C*4), 118.3 (py′-*C*5), 57.6 (N*C*H$_2$-py), 56.8 (N*C*H$_2$-py′), 41.2 (*C*–(CH$_3$)$_3$) and 27.3 (C-(*C*H$_3$)$_3$); BPh$_4^-$ 164.7 (B-*C*1, J_{B-C} = 49.6 Hz), 136.7 (*C*2), 126.6 (*C*3), 122.7 (*C*4). ESI-MS (+ ion) Found 488.2 (100%), Calcd. 488.12 (100%) for [(bppapa)Zn(Cl)]$^+$, and matches theoretical isotope distribution.

Hydrolysis of 1 and bppapa. 1 (0.024 g, 0.0324 mmol) or bppapa (0.012 g, 0.0324 mmol) was dissolved in CD_3CN (0.6 cm^3) and mixed with a CD_3OD solution (0.1 cm^3) of $Me_4NOH·5H_2O$ (0.059 g, 0.324 mmol) at 323 K. ^{1}H NMR spectra of these mixtures were recorded at various times for a period of 8 h for **1** and 10 days for bppapa. The amide cleavage reaction was confirmed comparing the ^{1}H NMR spectra of the final reaction mixtures with those obtained on mixing [(bpapa)Zn](PF$_6$)$_2$ (0.0324 mmol) or bpapa[29] (0.0324 mmol) in CD_3CN (0.6 cm^3) with a CD_3OD (0.1 cm^3) solution of $Me_4NOH·H_2O$/trimethylacetic acid (0.324 : 0.324 mmol) (Figs. S4 and S5 (provided as ESI†)). ESI-MS (+ ion) analysis of the reaction mixtures showed prominent isotope ion clusters at *m*/*z* 409.5 (in the hydrolysis of **1**) and 306.1 (in the hydrolysis of bppapa) consistent with [(bpapa^{-1})Zn(NCCH$_3$)]$^+$ and [(bpapa)H]$^+$ cations, respectively.

X-Ray crystallography

Crystals suitable for X-ray diffraction studies were grown by slow evaporation of bppapa in diethyl ether, [(bppapa)Zn](PF$_6$)$_2$ **1** in methanol/chloroform (1 : 1), [(bpapa)Zn(Cl)](BPh$_4$) **2′** in CH_3CN/H_2O (1 : 1) at room temperature.

Intensity data for bppapa and **2′** were collected at 150 K using a Bruker AXS SMART APEX area detector diffractometer with graphite-monochromated Mo-Kα radiation (λ = 0.71073 Å). The structures were solved by direct methods and refined to convergence against F^2 data using the SHELXTL suite of programs.[30] Data were corrected for absorption applying empirical methods using the program SADABS,[31] and the structures were checked for higher symmetry using the program PLATON.[32] All non-hydrogen atoms were refined anisotropically; hydrogen atoms were placed in idealised positions and treated using a riding model with fixed isotropic displacement parameters. In **2′**·CH_3CN the N–H hydrogen was located in the difference map and refined isotropically.

Intensity data for **1** were collected at 150 K on a Stoe Stadi-4 diffractometer operating with Cu-Kα radiation (λ = 1.54184 Å). A face-indexed absorption correction was applied following optimisation of the crystal habit against a set of ψ-scans (Stoe XSHAPE).[33] The structure was solved by direct methods, and refined by full-matrix least squares against F^2. All non-hydrogen atoms were refined with anisotropic displacement parameters with hydrogen atoms placed in idealised positions. Although the fluoride atoms which form part of the PF$_6^-$ anions adopt rather large anisotropic displacement parameters, they are not unreasonably so, and an ordered model is presented here. It was clear from electron density difference maps that the structure contained a small region of disordered solvent, probably methanol, based around a crystallographic inversion centre. This region was treated in the manner described by van der Sluis and Spek.[34] It comprises 9.25 e$^-$ per formula unit, which equates to approximately 0.5 methanol molecules; the values of *F*(000), μ, density *etc*. have been calculated on the basis of this assumption.

CCDC reference numbers 203672–203674.

See http://www.rsc.org/suppdata/dt/b3/b301651j/ for crystallographic files in CIF or other electronic format.

Acknowledgements

We gratefully acknowledge the EPSRC (GR/R25743/01), the Royal Society (RSRG: 22702), the Nuffield Foundation (NAL/00286/G) and The University of Edinburgh for funding. We would like to thank Dr Andy Parkin for processing X-ray data and Mr John Millar for collecting some of the NMR spectra.

References and notes

1 (*a*) W. N. Lipscomb and N. Sträter, *Chem. Rev.*, 1996, **96**, 2375; (*b*) R. Krämer, *Coord. Chem. Rev.*, 1999, **182**, 243; (*c*) E. L. Hegg and J. N. Burstyn, *Coord. Chem. Rev.*, 1998, **173**, 133.
2 (*a*) D. W. Christianson and W. N. Lipscomb, *Acc. Chem. Res.*, 1989, **22**, 62; (*b*) H. Kim and W. N. Lipscomb, *Biochemistry*, 1991, **30**, 8171.
3 X. Iturrioz, R. Rozenfeld, Z. A. Michaud, P. Corvol and C. Llorens-Cortes, *Biochemistry*, 2001, **40**, 14440.
4 A. D. Pannifer, T. Y. Wong, R. Schwarzenbacher, M. Renatus, C. Petosa, J. Bienkowska, D. B. Lacy, R. J. Collier, S. Park, S. H. Leppla, P. Hanna and R. C. Liddington, *Nature (London)*, 2001, **414**, 229.
5 U. Baumann, S. Wu, K. M. Flaherty and D. B. McKay, *EMBO J.*, 1993, **12**, 3357.
6 H. M. Holden, D. E. Tronrud, A. F. Monzingo, L. H. Weaver and B. W. Matthews, *Biochemistry*, 1987, **26**, 8542.
7 W. C. Parks and R. P. Mecham, *Matrix Metalloproteinases*, Academic Press, San Diego, 1998.
8 J. C. Mareque Rivas, H. Schwalbe and S. J. Lippard, *Proc. Natl. Acad. USA*, 2001, **98**, 9478.
9 (*a*) G. Aullón, D. Bellamy, L. Brammer, E. A. Bruton and A. G. Orpen, *Chem. Commun.*, 1998, 653; (*b*) J. C. Mareque Rivas and L. Brammer, *Inorg. Chem.*, 1998, **37**, 4756; (*c*) A. L. Gillon, G. R. Lewis, A. G. Orpen, S. Rotter, J. Starbuck, X. Wang, Y. Rodríguez-Martín and C. Ruiz-Perez, *J. Chem. Soc., Dalton Trans.*, 2000, 3897; (*d*) L. Brammer, J. K. Swearingen, E. A. Bruton and P. Sherwood, *Proc. Natl. Acad. Sci. USA*, 2002, **99**, 4956.
10 (*a*) D. P. Bancroft, C. A. Lepre and S. J. Lippard, *J. Am. Chem. Soc.*, 1990, **112**, 6860; (*b*) K. J. Barnham, S. J. Berners-Price, T. A. Frenkiel, U. Frey and P. J. Sadler, *Angew. Chem., Int. Ed. Engl.*, 1995, **34**, 1874.
11 (*a*) C. E. MacBeth, A. P. Golombek, V. G. Young, Jr., C. Yang, K. Kuczera, M. P. Hendrich and A. S. Borovik, *Science*, 2000, **289**, 938; (*b*) A. Wada, H. Harata, K. Hasegawa, K. Jitsukawa, H. Masuda, M. Mukai, T. Kitagawa and H. Einaga, *Angew. Chem., Int. Ed.*, 1998, **37**, 798; (*c*) R. H. Crabtree, P. E. M. Siegbahn, O. Eisenstein, A. L. Rheingold and T. F. Koetzle, *Acc. Chem. Res.*, 1996, **29**, 348; (*d*) A. L. Canty and G. van Koten, *Acc. Chem. Res.*, 1995, **28**, 406; (*e*) W. Yao and R. H. Crabtree, *Inorg. Chem.*, 1996, **35**, 3007; (*f*) D.-H. Lee, H. J. Kwon, B. P. Patel, L. M. Liable-Sands, A. L. Rheingold and R. H. Crabtree, *Organometallics*, 1999, **18**, 1615.
12 C. J. Boxwell and P. H. Walton, *Chem. Commun.*, 1999, **17**, 647.
13 M. Wall, B. Linkletter, D. Williams, A.-M. Lebuis, R. C. Hynes and J. Chin, *J. Am. Chem. Soc.*, 1999, **121**, 4710.
14 E. Kövári and R. Krämer, *J. Am. Chem. Soc.*, 1996, **118**, 12704.
15 (*a*) D. K. Garner, S. B. Fitch, L. H. McAlexander, L. M. Bezold, A. M. Arif and L. M. Berreau, *J. Am. Chem. Soc.*, 2002, **124**, 9970; (*b*) D. K. Garner, R. A. Allred, K. J. Tubbs and L. M. Berreau, *Inorg. Chem.*, 2002, **41**, 3533; (*c*) L. Berreau, M. M. Makowska-Grzyska and A. M. Arif, *Inorg. Chem.*, 2001, **40**, 2212.
16 B. L. Vallee and D. S. Auld, *Proc. Natl. Acad. Sci. USA*, 1990, **87**, 220 and references therein.

17 C. K. Johnson, ORTEP II, Report ORNL-5138, Oak Ridge National Laboratory, Oak Ridge, TN, 1976.
18 L. M. Berreau, M. M. Makowska-Grzyska and A. M. Arif, *Inorg. Chem.*, 2000, **39**, 4390.
19 F. H. Allen, O. Kennard, D. G. Watson, L. Brammer, A. Guy Orpen and R. Taylor, *J. Chem. Soc., Perkin Trans. 2*, 1987, S1.
20 H. Adams, N. A. Bailey, D. E. Fenton and Q.-Y. He, *J. Chem. Soc., Dalton Trans.*, 1997, 1533.
21 (*a*) J. C. Mareque Rivas, D. Zhao and L. Brammer, *Inorg. Chem.*, 1998, **37**, 5512; (*b*) J. C. Mareque Rivas and L. Brammer, *Coord. Chem. Rev.*, 1999, **183**, 43.
22 The chemical shift of the two H6 protons of **2′**, which are equivalent in solution, does not change upon heating to 50 °C (Fig. S3 (see ESI †)).
23 A. V. Iogansen, G. A. Kurkchi, V. M. Furman, V. P. Glazunov and S. E. Odinokov, *Zh. Prikl. Spektrosk.*, 1980, **33**, 460.
24 **2′** and $AgPF_6$ (1 equiv.) were incubated at 50 °C for 24 h in CD_3CN. The ^1H NMR and ESI-MS (+ ion) spectra of the resulting compound were identical to those of **1**.
25 (*a*) J. T. Groves and R. R. Chambers, Jr., *J. Am. Chem. Soc.*, 1984, **106**, 630; (*b*) J. Chin, V. Jubian and K. Mrejen, *J. Chem. Soc., Chem. Commun.*, 1990, 1326.
26 One possible effect of amide co-ordination to the zinc(II) center is activation towards nucleophilic attack (see text and Scheme 2). The reaction of **1** with $Me_4NOH·5H_2O$ (1 equiv.) at 50 °C in CD_3CN/CD_3OD (6 : 1) results in amide hydrolysis in a yield of *ca*. 95% after 8 hours (Figs. S4 and S5 (see ESI †)). The reaction of bppapa under identical conditions affords the hydrolysed product, *N,N*-bis-(2-pyridylmethyl)-*N*-(6-amino-2-pyridylmethyl)amine (bpapa) in a yield of *ca*. 95% after 10 days. Studies directed at fully establishing the mechanism of amide hydrolysis of bppapa and related ligands are currently in progress.
27 W. L. F. Armarego and D. D. Perrin, *Purification of Laboratory Chemicals*, Butterworth-Heinemann, Oxford, 4th edn., 1997.
28 L. M. Berreau, S. Mahapatra, J. A. Halfen, V. G. Young, Jr. and W. B. Tolman, *Inorg. Chem.*, 1996, **35**, 6339.
29 J. C. Mareque-Rivas, E. Salvigni, R. Torres Martín de Rosales and S. Parsons, in preparation.
30 G. M. Sheldrick, SHELXTL 97, University of Göttingen, Germany, 1997.
31 (*a*) G. M. Sheldrick, SADABS, Empirical absorption correction program, University of Göttingen, 1995, based upon the method of Blessing; (*b*) R. H. Blessing, *Acta Crystallogr., Sect. A*, 1995, **51**, 33.
32 A. L. Spek, PLATON, *Acta Crystallogr., Sect. A.*, 1990, **46**, C34.
33 Stoe and Cie, GmbH, IPDS, 2.87 Software Manual, Darmstadt, Germany.
34 P. van der Sluis and A. L. Spek, *Acta Crystallogr., Sect. A.*, 1990, **46**, 194.